cogent engineering

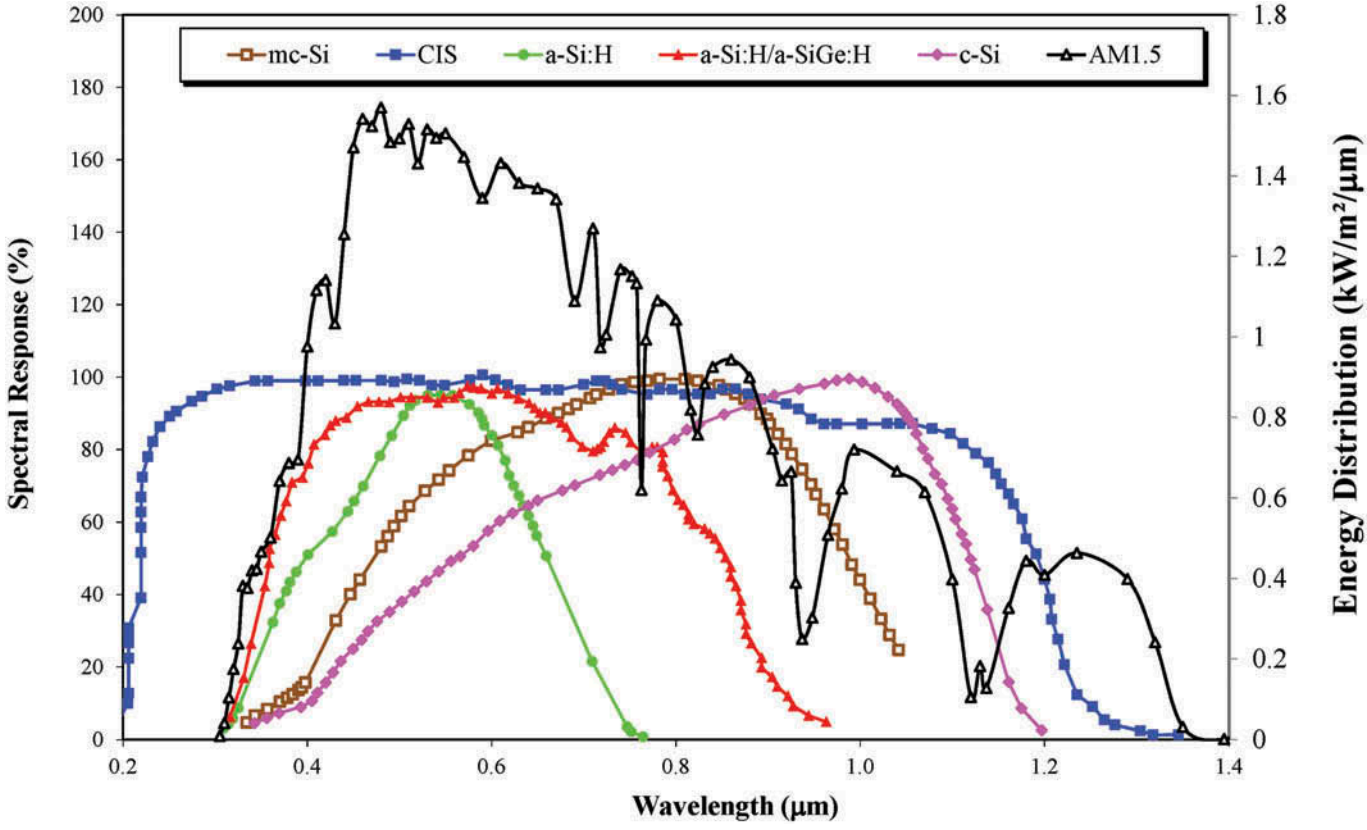

ELECTRICAL & ELECTRONIC ENGINEERING | RESEARCH ARTICLE

Blue skies and red sunsets: Reliability of performance parameters of various p-n junction photovoltaic module technologies

Edson L. Meyer and Ochuko K. Overen

Cogent Engineering (2019), 6: 1691805

cogent engineering

ELECTRICAL & ELECTRONIC ENGINEERING | RESEARCH ARTICLE

Blue skies and red sunsets: Reliability of performance parameters of various p-n junction photovoltaic module technologies

Edson L. Meyer[1] and Ochuko K. Overen[1]*

Received: 06 August 2019
Accepted: 06 November 2019;First Published: 12 November 2019

*Corresponding author: Ochuko K. Overen, Fort Hare Institute of Technology, University of Fort Hare, Alice 5700, South Africa
E-mail: ooveren@ufh.ac.za

Reviewing editor:
N. Prabaharan, Shanmugha Arts Science Technology and Research Academy, India

Additional information is available at the end of the article

Abstract: This research presents, discusses and compares the reliability of the performance characteristics of six different p-n junction photovoltaic module technologies under varying operating conditions. The six module technologies are: $CuInSe_2$ (CIS), a-Si:H, a-Si:H/a-SiGe:H/a-SiGe:H (a-SiGe:H), edge-defined film-fed growth silicon (EFG-Si), multi-crystalline silicon (mc-Si) and single crystalline silicon (c-Si). A simple but accurate method is then used to determine the modules' qualities. The effect of temperature on module performance is then investigated and results compared. Here it was found that the lower quality thin-film technologies are not as temperature dependent as their crystalline counterparts. The influence of irradiance on module performance was also measured and compared for the different technologies. The a-Si:H technology was found to be at least 16% more efficient than the other module technologies at 169 W/m^2. Under actual outdoor operating conditions, however, the reliability of the STC measurements is no longer useful. CIS performs relatively better at high air-mass values, corresponding to times when the sun is lower in the sky, that is, red sunsets. Under these outdoor conditions, irradiance, temperature and spectral changes affect module performance and this research successfully motivates the importance of considering all

Edson L. Meyer

ABOUT THE AUTHORS

Edson L. Meyer obtained his PhD in Physics at the University of Port Elizabeth, South Africa in 2002 and has been actively involved in renewable energy research for 23 years. His current research deals with various aspects of solar PV and solar thermal, dye-sensitized and perovskite solar cells, with solar water heaters, grid-connected PV, biomass gasification and biogas digestion. He is currently the Executive Director of the Fort Hare Institute of Technology where he resides as a full professor with a C rating from the National Research Foundation.

Ochuko K. Overen joins the University of Fort Hare, Alice, South Africa in 2010 for his research career, where he went on to obtain his PhD in Physics. Dr Overen is a recipient of the National Research Foundation (NRF) of South Africa 2019 Innovation postdoctoral fellowship grant award. He is a professional member of the South African Institute of Physics (SAIP).

PUBLIC INTEREST STATEMENT

When the sun travels across the sky from sunrise, noon and to sunset, the content of the light is preferentially scattered by various gases and particles in the atmosphere. The result is blue skies since blue light (lower wavelength) is scattered more and red sunsets, the time of day when only longer wavelengths (red light) is reaching the observer. Just like the human eye, solar cells and module comprising materials of different energy bandgap respond differently to different times of day when the spectrum or content of light is different. This study shows that the spectral effect on the performance of PV modules cannot be ignored when comparing different technologies. In fact, some technologies like $CuInSe_2$ and c-Si technologies become more efficient toward sunset as compared to their performance around noon. The fundamental truth portrayed by this study is that STC measurement alone cannot reliably give a comparison of the performance of different module technologies.

three factors to be of equal importance when analysing the reliability of outdoor performance parameters of photovoltaic modules.

Subjects: Semiconductors; Nondestructive Testing; Renewable Energy; Solar energy

Keywords: photovoltaic modules; reliability of performance parameters; spectral response; irradiance effect; thin film and temperature effect

1. Introduction

Solar cells, like the human eye, respond differently to different colours of light or more precisely to the content of sunlight. With the advent of new technologies like single or tandem junction solar cells, it is imperative to understand how cells modules perform under varying sets of operating conditions. Therefore, the notion that a single measurement at a single set operating conditions (like standard test conditions-STC) is sufficient to classify and compare modules is fallacious. This is then also the motivation behind this research, where the reliability of the performance parameters of various p-n junction photovoltaic (PV) modules were evaluated. In particular, the effect of temperature, irradiance and spectral distribution on module performance was investigated. This paper shows that the shift in wavelength as the sun traverse from blue skies to red sunset, has a significant impact on the performance of different technologies that may not be evident from the measurement at STC.

Standard test conditions (STC: 1000 W/m^2 irradiance, 25°C cell temperature and AM 1.5 global spectrum) were adopted for the purpose of comparing photovoltaic (PV) cells and modules under specific reference conditions. The irradiance represents peak sunlight and the 25°C cell temperature is representative of room temperature in most laboratories. The air mass (AM 1.5) is the ratio of the atmospheric mass in the actual observer-sun path to the mass that would exist if the observer were at sea level, at standard barometric pressure with the sun directly overhead. If, however, PV cells and modules are operating outdoors, meteorological conditions are usually far from STC. Under these outdoor conditions, STC module characteristics are no longer a reliable performance indicator. The three factors influencing module characteristics the most are temperature, irradiance and spectral changes. Knowledge of the influence of these factors on module performance is therefore essential, especially for system designers and consumers, to determine module suitability.

This research outlines the methodology for measuring the indoor performance under STC to establish a baseline. From varying the light intensity, a Isc—Vcc method (Meyer, 2017) was used to determine the quality of modules through ideality factor n, and dark saturation current I_o. Changing the operating temperature under indoor conditions, the temperatrure dependence of Isc, Voc and Pmax were determined. Then efficiency at various irradiance levels was determined. These test modules were then placed outdoor where the performances were measured under varying spectral distributions. The results show that measurements at STC alone may yield inaccurate comparison results since the effect of varying spectrum cannot be neglected when comparing PV modules.

In this research, the quality of the modules is established using light current-voltage (*I*-*V*) measurements, and measuring short-circuit current and open-circuit voltage (I_{sc}-V_{oc}) under various irradiance levels. From both methods it was found that the EFG-Si module is the most efficient (11.3%) and has the best quality cells (n = 1.07). Temperature dependence measurements revealed that the high quality crystalline modules are more sensitive to temperature variations. Irradiance measurements under reduced light in the solar simulator showed that at 169 W/m^2, the a-Si:H is 16% more efficient than the other modules. But under actual operating conditions, the CIS performs relatively better at high air mass values, i.e, when the sun is lower in the sky. Comparison of performance on the same day at solar noon and close to sunset revealed that the efficiency of the CIS and crystalline modules increased towards sunset.

2. Methodology

Photovoltaic (PV) modules used in this study comprise different technologies including thin-film polycrystalline, thin-film amorphous and crystalline materials. Of the nine modules used in this study, results obtained from six representing the different technologies, will be presented and discussed. An assessment procedure (Meyer & Van Dyk, 2004) was used to assess module performance and obtain performance parameters. The assessment procedure includes amongst others, comprehensive visual inspection, quantitative quality measurements, temperature measurements, effect of irradiance determination and outdoor performance measurements. The modules were initially subjected to the assessment procedure. These results were then used as a baseline for subsequent future measurements. Results obtained in the study indicate that all thin-film modules degraded over the test period. It was, however, found that some of the degradation modes might have been caused by the assessment procedure (Meyer & Van Dyk, 2004). For the sake of fairness, this research therefore mainly deals with comparison of results obtained from the initial indoor assessment, prior to outdoor deployment. Results obtained from measurements taken while the modules were deployed outdoors are also presented and compared. Actual performance, degradation and analysis thereof for CIS and a-Si modules are discussed elsewhere (Adrada Guerra, Amador Guerra, Orfao Tabernero, & de la Cruz García, 2017; Carr & Pryor, 2004; Del Cueto, Rummel, Kroposki, Osterwald, & Anderberg, 2008; Meyer, 2017; Vázquez & Rey-Stolle, 2008).

3. Indoor performance characteristics

Standard test conditions provide an excellent means of comparing the performance parameters of PV modules. Figure 1 shows the I-V characteristics of the six modules representing the different technologies.

The I-V characteristics were measured initially before outdoor deployment with a xenon-pulsed solar simulator at STC.

Evident from the figure is the fact that the modules have different ratings and characteristics.

Table 1 lists the different module technologies, the manufacturer's rated power and parameters obtained from the I-V characteristics in Figure 1. Parameters obtained include maximum power

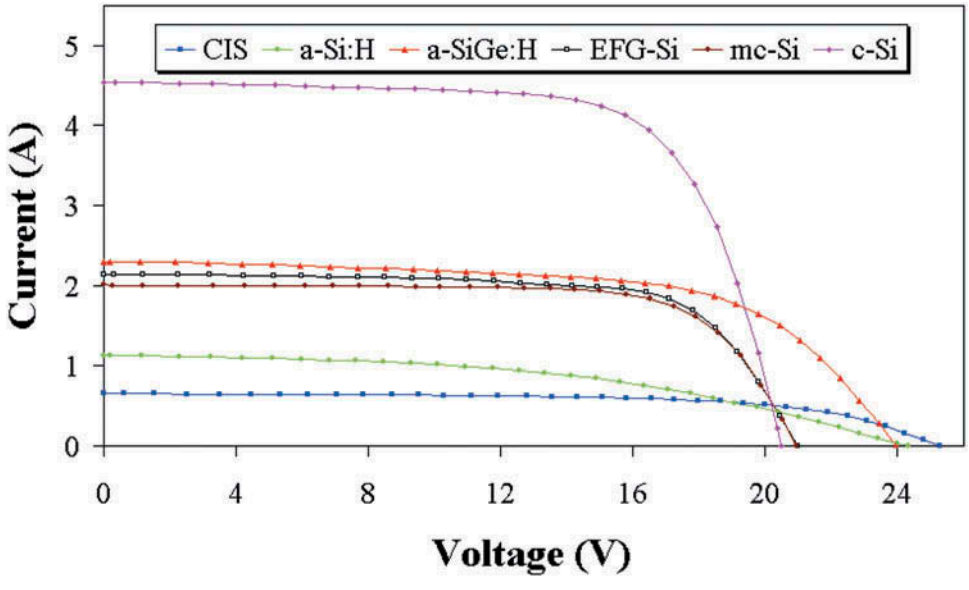

Figure 1. I-V characteristics of the different PV modules measured at STC before outdoor deployment.

Table 1. Module technology, rated power and parameters obtained from the I-V characteristics in Figure 1

Module	P_{max} Rated (W)	P_{max} @ STC (W)	I_{sc} (A)	V_{oc} (V)	R_s (Ω)	*FF* (%)	η(%)
CIS	10.0	10.76	0.65	25.26	5.99	65	9.19
a-Si:H	14.0	12.98	1.15	24.47	9.76	46	4.41
a-SiGe:H	32.0	34.72	2.30	23.94	1.94	63	7.69
EFG-Si	32.0	31.64	2.14	20.98	1.60	70	11.3
mc-Si	30.0	30.62	2.01	20.94	1.54	73	11.0
c-Si	65.0	64.45	4.49	20.45	0.70	70	10.7

(P_{max}), short-circuit current (I_{sc}), open-circuit voltage (V_{oc}), series resistance (R_s), fill factor (FF) and aperture area efficiency (η).

From the Table it is evident that the c-Si module has the highest P_{max}, which is also close to its rated power. Also, although it has the lowest R_s it does not have the highest FF or η. The EFG-Si, on the other hand, with the highest conversion efficiency, does not have the highest FF. This is attributed to the cracked cell in the EFG-Si module that was observed in the initial visual inspection (Meyer & Van Dyk, 2004). The mc-Si module has the highest FF. The relatively lower FF of the thin-film modules (CIS, a-Si:H and a-SiGe:H) is attributed to the higher V_{oc} and R_s values. Comparing I_{sc} of the thin-film modules, the higher I_{sc} of the a-SiGe:H module is attributed to a larger cell area and the fact that it employs triple-junction technology, where the different junctions absorb different parts of the AM 1.5 global spectrum. Considering the conversion efficiencies, it is clear that the EFG-Si module is the best, while the a-Si:H module is the worst.

Figure 2 shows the normalized I-V characteristics of the six modules. These normalized I-V characteristics enable direct comparison of the different module technologies.

It is clear from the figure that the thin-film module qualities are inferior to that of the crystalline modules. As opposed to the values listed in Table 1, Figure 2 suggests that the mc-Si should have the best efficiency. Considering, however, that the cracked cell in the EFG-Si module lowers the current in the top part of the I-V characteristic, it is clear why the EFG-Si module is not portrayed

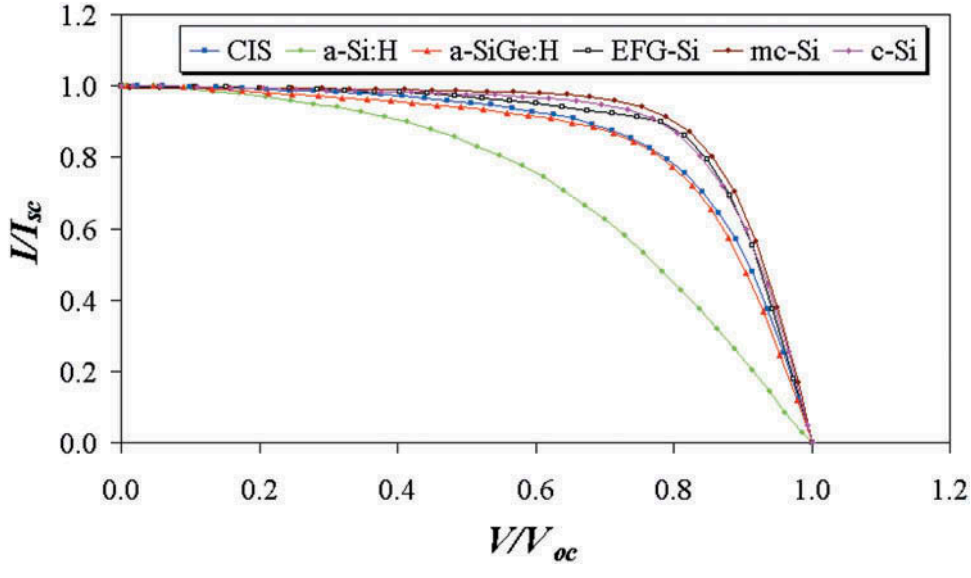

Figure 2. Normalized I-V characteristics of the six module technologies used.

here as the best module. A further investigation of the quality of the module cells has been conducted and is discussed in the next section.

3.1. Module quality

A method employing I_{sc} and V_{oc} measurements (Meyer, 2017) was used to determine the quality of each module and its constituent cells. For a solar cell or module, the current-voltage characteristics are governed by:

$$I = I_{ph} - I_{01}\left(e^{\frac{q(V-IR_s)}{kT}} - 1\right) - I_{02}\left(e^{\frac{q(V-IR_s)}{nkT}} - 1\right) - \frac{V - IR_s}{R_{sh}} \quad (1)$$

where: I_{ph} is the photogenerated current, R_s is the cell's series resistance and R_{sh} the shunt resistance.

Now, assuming no ideal recombination, the term containing the saturation current I_{01}, in Equation (1) can be neglected. Assuming also that $I_0 \ll I_{sc} \sim I_{ph}$ and $R_{sh} \gg V_{oc}/I_{sc}$, V_{oc} (I = 0) can be expressed as:

$$V_{oc} = \frac{nkT}{q}(\ln I_{sc} - \ln I_0) \quad (2)$$

where: I_0 = saturation current corresponding to generation and recombination of electrons and holes in the space-charge-region (SCR), i.e., non-ideal recombination;

n = ideality factor > 1;

Figure 3 shows V_{oc} as a function of I_{sc} for the six module technologies. A plot of V_{oc} against $\ln I_{sc}$ from Equation (2) is usually linear and yields values for the ideality factor (n) and reverse saturation current (I_0) (Meyer, 2017). If the plot is sub-linear, the assumptions for Equation (2) are not true and the module is expected to have cells with low shunt resistances.

Different values for V_{oc} and I_{sc} were obtained by measuring I-V characteristics at various irradiance levels inside the solar simulator. Module temperatures were maintained at 25°C. All measurements presented here were taken before outdoor deployment.

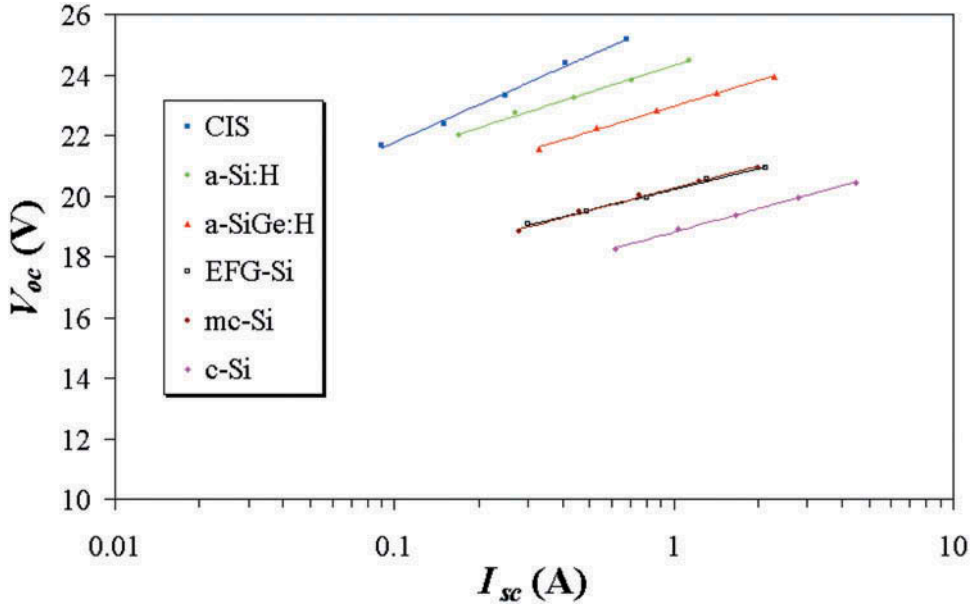

Figure 3. V_{oc} vs. I_{sc} yielding ideality factor and reverse saturation current of the various module technologies.

Table 2 lists the parameters (n and I_0) obtained from the logarithmic fits to the data in Figure 3 for the single junction modules only. The closer n is to unity, the better the quality of the module cells. Also, n > 1 implies that apart from ideal recombination in the quasi-neutral p- and n-regions, non-ideal recombination also takes place in the Space Charge Region of the p-n junction (Calzolari & Graffi, 1972; Zhukov, 2016).

From Table 2 it is evident that the EFG-Si module has the best quality cells as suggested by Table 1. The relatively higher n for the thin-film modules reveals that their cell quality is lower than the crystalline cells. It also implies that non-ideal recombination takes place especially for the a-Si:H module with n close to 2. The high I_0 of the CIS module is due to the fact that the CIS module showed shunting behaviour and the method of determining n and I_0 is therefore inaccurate for this module. In general, the lower quality of the thin-film modules is mainly due to less stringent manufacturing processes used in an attempt to reduce manufacturing costs.

Equation (1) was derived from the equation governing the I-V characteristics of conventional p-n junctions. This equation is different for the triple junction a-SiGe:H module. If, however, the equation for the single junction modules is applied to the a-SiGe:H module, n is found to be 1.44 per junction and I_0 is equal to 6.87 nA.

3.2. Temperature dependence

Elevated temperatures influence the performance of PV modules operating outdoors. A primary concern to system designers is the loss of performance due to increasing temperatures. In this section, the temperature coefficients of I_{sc}, V_{oc} and P_{max} are determined for the various module technologies. Heating the modules to a predetermined temperature, then placing them in the solar simulator and measuring I-V characteristics as the modules cool down uniformly inside the simulator allowed determination of all coefficients.

3.2.1. Short-circuit current

Figure 4 shows the temperature dependence of I_{sc} for the various technologies and Table 3 lists the corresponding temperature coefficient (α) in mA/°C. The percentage change per unit temperature (%/°C) was calculated with respect to I_{sc} measured at STC (25°C).

From Figure 4 and Table 3, it is evident that I_{sc} of all modules increases slightly with increase in temperature. This increase is due to the fact that the material bandgap, E_g, decreases with increase in temperature allowing lower energy photons to generate e-h pairs. Also, as temperature increases, the thermal velocity of charge carriers increases and effectively reduces the recombination probability of minority carriers (Dubey, Sarvaiya, & Seshadri, 2013; Mazer, 1997; Perraki & Tsolkas, 2013). The average temperature dependence of I_{sc} is in excellent agreement with the theoretical value of 0.06%/°C for Si (Singh & Ravindra, 2012). α for a-SiGe:H is also lower than that of a-Si:H. I_{sc} of the CIS module is the least dependent on temperature.

3.2.2. Open-circuit voltage

The main effect of increasing temperature is the reduction of voltage with increasing temperature. Figure 5 shows V_{oc} of the six module technologies as a function of temperature. The gradients of the best-fit lines shown in the figure yield the temperature coefficient for V_{oc} (β). These coefficients are listed in Table 4.

Table 2. Parameters (n and I_0) obtained for the various module technologies from V_{oc}-I_{sc} measurements. Data shown here are for the single junction technologies only

Module	CIS	a-Si:H	EFG-Si	mc-Si	c-Si
n	1.38	1.71	1.07	1.15	1.19
I_0(nA	486	5.47	1.28	5.82	40.7

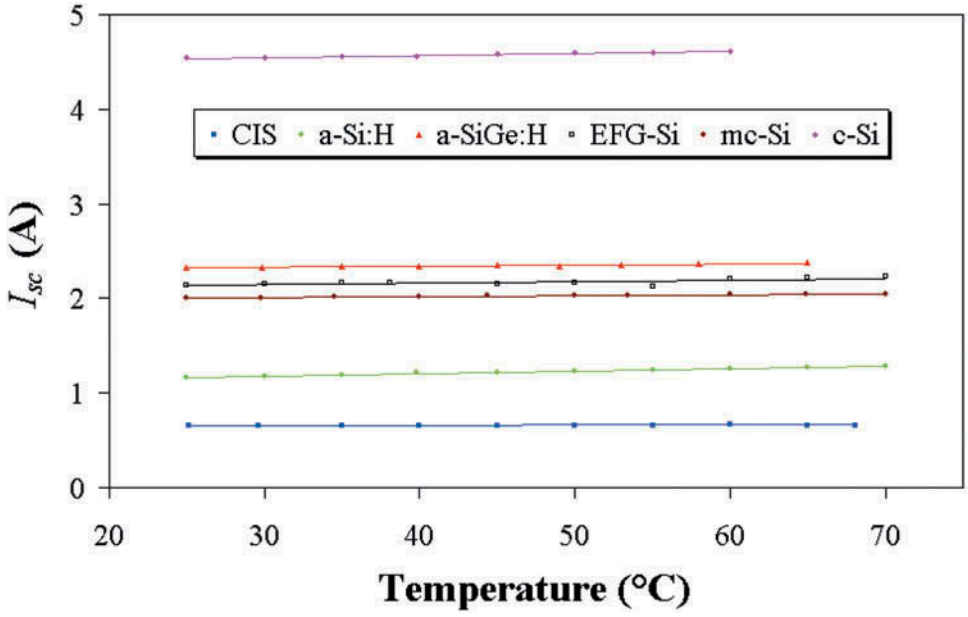

Figure 4. Temperature dependence of I_{sc} for the different module technologies.

Table 3. Temperature coefficients (α) of I_{sc} corresponding to the curves in Figure 4

Module	CIS	a-Si:H	a-SiGe:H	EFG-Si	mc-Si	c-Si
α(mA/°C)	0.06	2.70	1.20	1.70	0.90	2.10
α(%/°C)	0.01	0.23	0.05	0.08	0.04	0.05

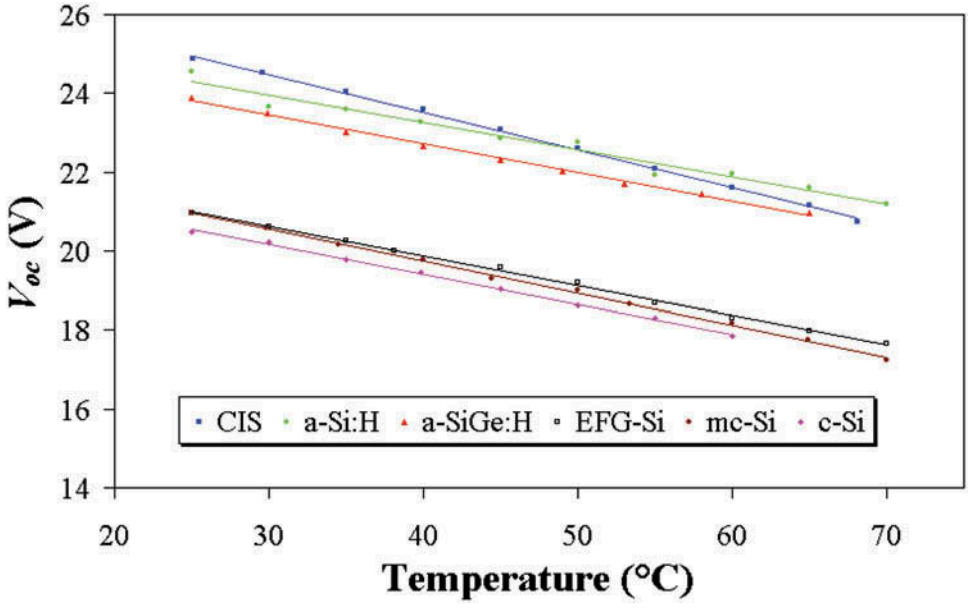

Figure 5. V_{oc} as a function of temperature for the different module technologies.

Table 4. Temperature coefficients (β) of V_{oc} corresponding to the curves in Figure 5

Module	CIS	a-Si:H	a-SiGe:H	EFG-Si	mc-Si	c-Si
β(mA/°C)	−96.0	−69.0	−73.1	−74.7	−81.4	−75.7
β(%/°C)	−0.39	−0.28	−0.31	−0.36	−0.39	−0.37

3.2.3. Maximum power

Although the PV module current increases slightly with increase in temperature, the decrease in voltage is more rapid, resulting in an overall decrease in P_{max} as temperature increases. Figure 6 shows the temperature dependence of P_{max} for the six module technologies. Since the temperature of PV modules operating outdoors are usually around 45°C, it is important to know exactly how a module's performance is affected by increasing temperatures. Table 5 lists the corresponding temperature coefficients (γ) of P_{max} for the different module technologies.

γ of the more efficient crystalline modules is much higher than that of the a-Si thin-film modules. This is a direct consequence of the high quality crystalline cells where a slight change in temperature has a huge effect on the material properties. This has also been found in previous studies (Omazic et al., 2019; Van Dyk, Meyer, Leitch, & Scott, 2000; Mattei et al., 2006; Ogbomo et al., 2018; Hishikawa et al., 2018; Adeeb et al., 2019; Eke and Bett, 2017; Islam et al., 2019). The positive γ of a-Si:H is attributed to improved photoconductivity at elevated temperatures (Friesen, Zaaiman, & Bishop, 1998).

3.2.4. Effect of irradiance

To determine the effect of irradiance on module performance when no spectral changes occur, I-V measurements were taken with the solar simulator while reducing the irradiance levels with natural screen filters (Hauser & Ahmed, 1998). Figure 7 shows the efficiencies of the six modules at various irradiance levels. The module temperatures were maintained at 25°C. In a previous study, it was shown that if a module's efficiency first increases as irradiance levels are reduced, current losses due to recombination are dominant, while if the efficiency only decreases, the dominant current dissipator at lower irradiance is shunting due to shunt paths (McMahon, Basso, & Rummel, 1996; Meyer & Van Dyk, 2000). Comparing the efficiencies at the lowest irradiance level (169 W/m^2), it is clear that the EFG-Si is the best performer. The crystalline modules perform better than the thin-film

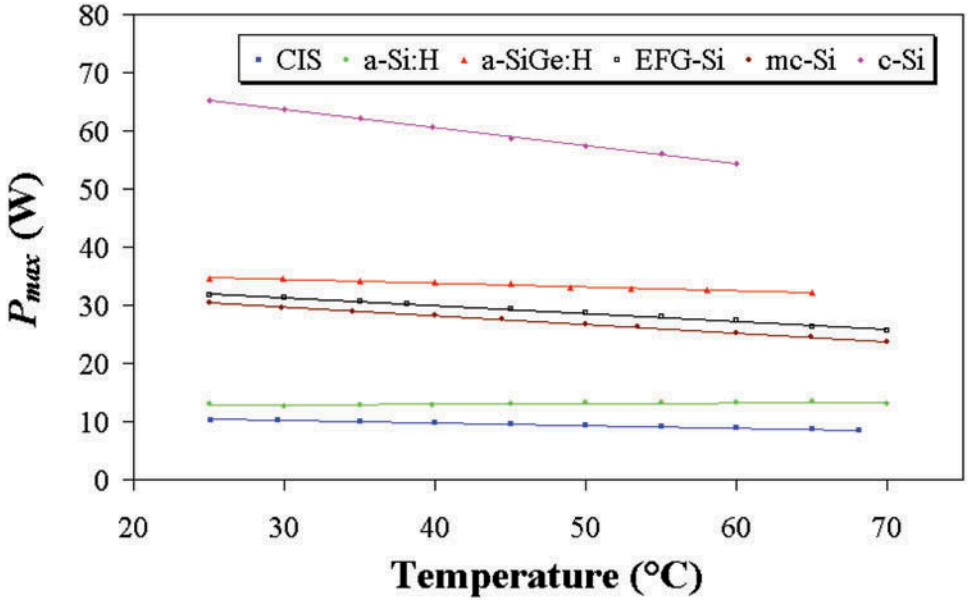

Figure 6. Temperature dependence of P_{max} for the different module technologies.

Table 5. Temperature coefficients (γ) of P_{max} corresponding to curves in Figure 6

Module	CIS	a-Si:H	a-SiGe:H	EFG-Si	mc-Si	c-Si
γ(mA/°C)	−41.7	10.3	−65.3	−139.0	−147.0	−309.1
γ(%/°C)	−0.41	0.08	−0.19	−0.44	−0.48	−0.47

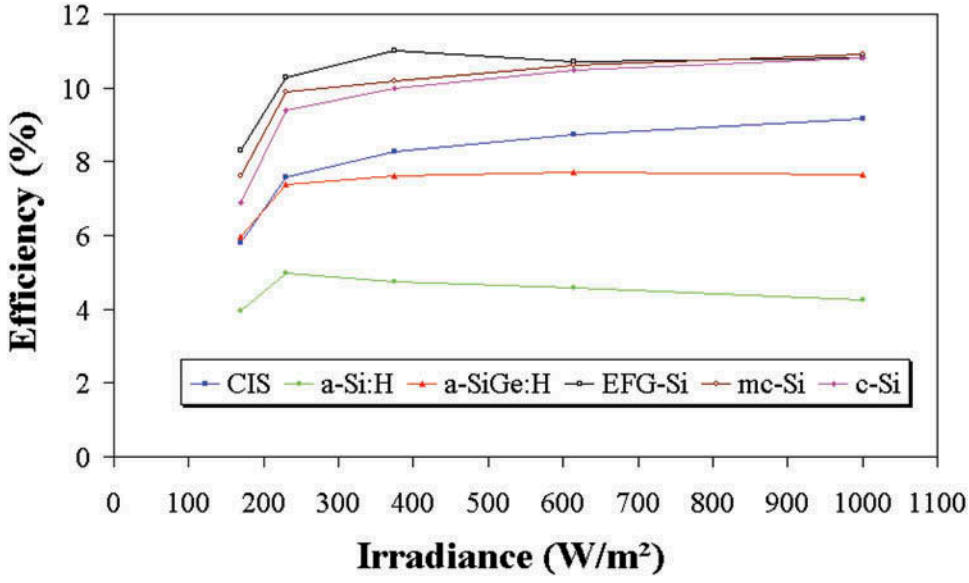

Figure 7. Aperture area efficiencies of the six modules as a function of irradiance.

modules at low irradiance. This is mainly due to the higher STC efficiencies of the crystalline modules. In order to explicitly compare all modules, the efficiencies of Figure 7 can be normalized to the STC efficiencies. Figure 8 shows the normalized efficiencies of the six modules at different irradiance levels. Effectively, the figure considers all modules to have the same STC efficiency. This allows a direct comparison of the relative efficiencies of the different technologies.

At the lowest irradiance level, the normalized efficiency of a-Si:H is at least 16% higher than all other technologies. The low normalized efficiency at 169 W/m^2 of CIS is attributed to its shunting behaviour (Das, De, & Mandal, 2019; Heise et al., 2011; Hoseinzadeh, Ghasemias, Bahari, & Ramezani, 2018, 2017; Paul, Smyth, & Zacharopoulos, 2019). Therefore, if all modules had the same STC efficiency, the a-Si:H technology would be the most efficient at irradiance levels below 1000 W/m^2. The a-SiGe:H technology is slightly more efficient than the EFG-Si technology at reduced irradiance levels.

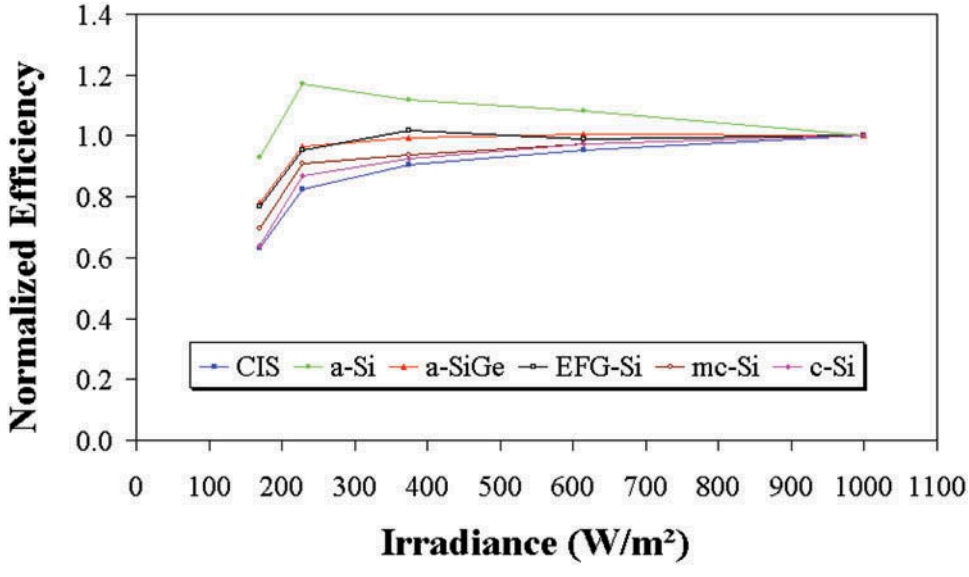

Figure 8. Normalized efficiencies of the six modules as a function of irradiance.

Under real outdoor operating conditions, the STC performance parameters become even less reliable as performance indicators. Reduced irradiance levels are usually associated with spectral changes, which may also influence module performance. The next section considers the effect of outdoor operating conditions on module performance.

3.3. Outdoor performance

3.3.1. Solar radiation monitoring system

Selected components of solar radiation were measured to conduct outdoor performance characterization of the PV modules. The selected solar radiation components include direct normal, global horizontal, and downward long-wave irradiance. To simultaneously monitor the above components, SOLYS Gear Drive (SGD) sun tracker was used. Figure 9 shows the SGD sun tracker and the various radiometer.

The SGD sun tracker comprises of a CHP 1 pyrheliometer, CGR4 pyrgeometer and two sets of CMP10 pyranometers. The SGD sun tracker was designed to offset the diurnal and seasonal movement of the earth (Mousazadeh et al., 2009). Hence, the payload was constantly pointed toward the sun. This was achieved by a sun sensor installed in the system. The sun sensor identifies the area in the sky with maximum solar intensity and directs the payload to that region. Besides the sun sensors, the tracker uses the coordinate and local time obtain by the integrated GPS antenna to track the daily movement of the sun. In this regard, the pyrheliometer used to measure direct normal irradiance was mounted on the payload. Thus, the pyrheliometer was also constantly pointed towards the sun. Whereas, the Pyrgeometer and two pyranometers located on the platform of the sun tracker, move about their axis. The pyrgeometer measures downward longwave radiation; in other words, the re-emitted (infrared) radiation of the atmosphere. While the pyranometer located at the extreme right end of the platform, measures diffused solar irradiance. As such, the shading assembly shields the pyrgeometer from direct short-wave solar radiation, which heats the pyrgeometer window. At the same time, it prevents direct solar radiation from the pyranometer. Combine direct, and diffuse irradiance on a horizontal plane was measured by the pyranometer located at the centre.

Like most Kipp&Zonen CMP series, the above mention radiometer uses a passive thermal sensing element called a thermopile to detect irradiance. The thermopile consists of thermocouple junction pairs connected in series. The measurement (hot) junction of one of the thermocouples absorbs

Figure 9. SOLYS gear drive dual-axis sun tracker containing various radiometers.

thermal radiation, increasing its temperature. The difference between the measurement and a fixed temperature reference (cold) junction produces a voltage directly proportional to the differential temperature created. This is known as the thermoelectric effect (Tang, Yang, He, & Qin, 2010). Although the construction of the thermopile differs from one radiometer to radiometer as well as from model to another, the principle of operation is the same. However, the sensitivity of a given radiometer thermopile depends on its physical properties (Kipp & Zonen, 2012). The specification of the radiometers used in the study is summarized in Table 6 and the profiles for September 14, which will be used later, shown in Figure 10.

The response time in Table 6 refers to the delay taken by the respective radiometer to respond to incident radiation. Also, the said response time is the time taken for the respective radiometer to deliver 95% of its measurement following a step-change in irradiance.

3.3.2. Effect of spectral changes

As the sun traverses the sky to and from the zenith during the day, the change in the solar altitude is characterized by the air mass (AM) number (m), which is defined as:

$$m = \csc\theta \tag{3}$$

where: m > 0 (air mass number, AM m);

θ = solar altitude (angle between sun and horizon).

Scattering of light by gas molecules in the atmosphere is proportional to λ^{-4}. This implies that blue light (λ ~ 0.4 μm) is scattered about eight to ten times more than red light (λ ~ 0.7 μm) (Nazeeruddin

Table 6. Specification of the radiometers used in this study

Radiometer	Specification		
	Spectral range (μm)	Sensitivity (μV/W/m^2)	Response time (s)
Pyheliometer	0.2 to 4	7 to 14	< 5
Pyrgeometer	4.5 to 42	5 to 10	< 18
Pyranometer	0.3 to 2.8	7 to 14	< 5

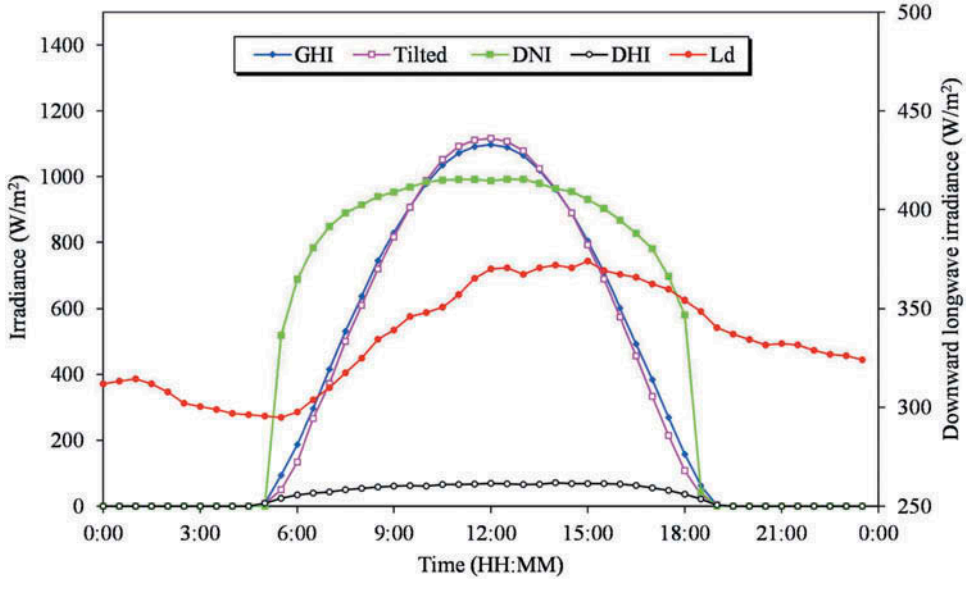

Figure 10. Selected components of solar radiation on September 14.

et al., 1993). During daytime, light from the sun appears yellow-white and the sky (not towards the sun) is perceived as blue. Towards sunset, when the sun is further away from the observer (higher AM), scattering will remove blue light preferentially, with the sun and sky appearing red. Therefore, high air mass numbers are associated with a spectral content dominated by long wavelength photons. Consequently, higher solar cell bandgap materials are less efficient under these high AM conditions. Figure 11 shows I_{sc} normalized to I_{sc} at AM 1.5 for the various module technologies. The values for I_{sc} were simulated with Sandia's Solar Design Studio software (S. D. Studio, 2000).

From the figure it is clear that the crystalline and CIS technologies do not have a strong dependence on AM. The two a-Si technologies do, however, depend strongly on AM. At AM 1.0, both a-Si technologies perform relatively better than their crystalline counterparts. At higher AM values, however, the normalized I_{sc} of a-Si decreases significantly. At these higher AM values, CIS performs better than the other modules.

This is attributed to the combination of wide and narrow bandgaps of the ZnO and $CuInSe_2$ forming the heterojunction. The wide bandgap ZnO being responsible for absorption of the shorter wavelength photons while the $CuInSe_2$ absorber layer is more responsive to longer wavelength photons. The ZnO/$CuInSe_2$ solar cell responds better to longer wavelength photons than the c-Si. This means that at higher AM values (representative of longer wavelength photons) when the sun is lower in the sky or on cloudy days, the CIS solar cell may become more efficient than the c-Si cell.

The a-SiGe:H module has the advantage of the spectral splitting technology, which is optimized for the low AM values. At high AM values (long photon wavelengths), however, the a-Si:H/a-SiGe:H module is less efficient. Since the spectral content consists mainly of low energy photons at the high AM values, the three series connected junctions of the a-SiGe:H module are mismatched resulting in reduced efficiencies.

Other research groups (Dai, Huang, He, Hui, & Bai, 2019; Eke & Senturk, 2013; King, Kratochvil, & Boyson, 2000; Nazeeruddin et al., 1993; Rodziewicz, Zabkowska-Waclawek, & Zdano-wicz, 2001; S. D. Studio, 2000; Santhakumari & Sagar, 2019) also support the fact that triple junction modules should be less efficient at high AM values. This is, however, contrary to results of Van Cleef, Lippens, and Call (2001), who report that the a-Si:H/a-SiGe:H modules, when deployed outdoors, have approximately 40% higher efficiencies at irradiance levels of 50–100 W/m^2 compared to other solar cell technologies like c-Si and $CuInSe_2$. This result is attributed to "the spectral splitting capability" of the module, "especially at lower irradiance levels and under diffuse light." Again, this is not in accordance with what is expected from spectral splitting theory, Figure 11, and the normalized efficiencies as a function of irradiance depicted in Figure 8. Evident from the figure though, is the fact that spectral changes do influence the performance of PV modules, though some more than others, and STC performance indicators are not reliable.

The behaviour of these solar cell technologies can be ascribed to their respective optical absorption coefficients, the wavelength range of their spectral response, and finally how aligned or mis-aligned these are with the solar spectrum and associated air mass.

The absorption coefficient, α, depends, therefore, on the semiconductor band gap, E_g, and is approximated by (Rodziewicz et al., 2001; Sze & Ng, 2006):

$$\alpha = A * (h\nu - E_g) \tag{4}$$

for allowed transitions of valence electron to the conduction band. In this equation, A* is a constant equal to 2 × 104 if α is expressed in cm^{-1} and hν and E_g in electron volt (eV). The

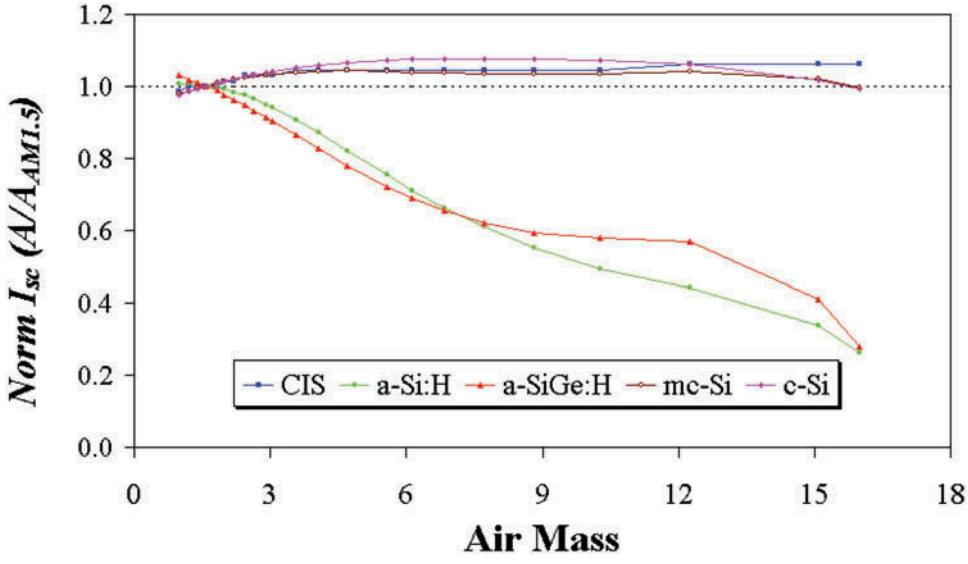

Figure 11. Normalized I_{sc} of the different technologies used in this study.

dependence of α on photon energy, hv, suggests that the solar cell will respond differently to different spectral distributions as is observed in Figure 11.

Figure 12 shows the AM1.5 spectrum superimposed on the spectral response of the 5 modules used in this study (Rodziewicz et al., 2001).

As the solar spectrum moves away from AM1.5, the spectrum experienced by the modules red-shifts towards the longer wavelengths. Clearly in the infrared region, around 800 nm, the CIS, crystalline and multi-crystalline modules still increase towards its 100% spectral response, while the a-Si based modules are either non-responsive (a-Si:H) or decreasing in response (a-SiGe:H).

3.3.3. PV module outdoor performance

While the modules were deployed outdoors, I-V characteristics were measured usually around solar noon with an automated I-V tracer. For the sake of clarity, the EFG-Si and mc-Si have been omitted

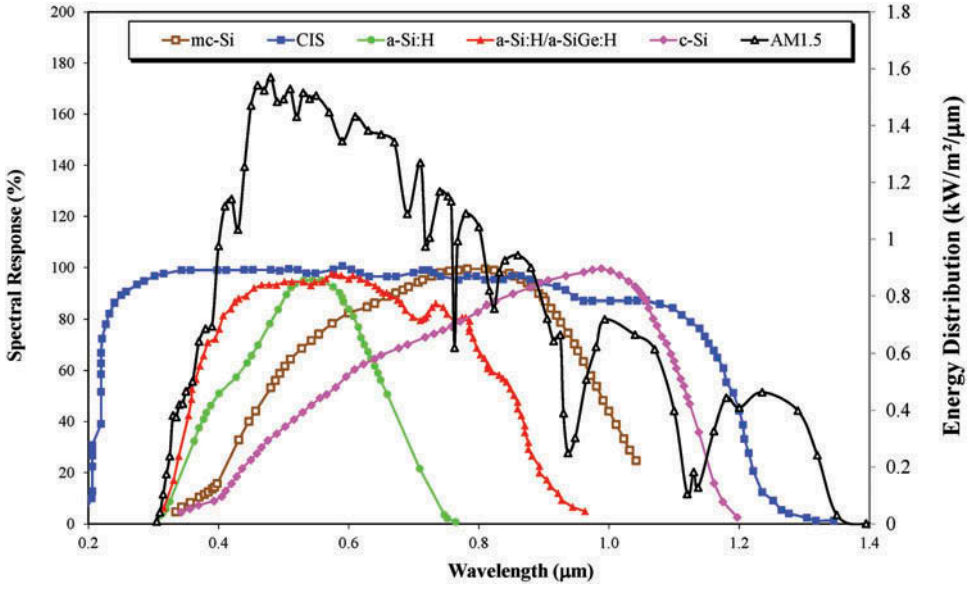

Figure 12. AM1.5 spectrum superimpose on the spectral response of the 5 modules used in this study; adapted from (Rodziewicz et al., 2001).

from this discussion (both modules showed similar behaviour as the c-Si module). Figure 13 shows the normalized I-V characteristics of four of the six module technologies used in this experiment. These I-V characteristics were measured on September 14 at 12 h30. This is around solar noon (AM close to unity) and the irradiance was relatively constant at 1100 W/m^2. The average back-of-module temperature was 35°C. From the figure it is clear that the c-Si module has the best relative I-V characteristic of the four modules. To consider the actual behaviour of these modules under outdoor conditions, no corrections were made for temperature or irradiance. Note that the normalized I-V characteristic of the a-SiGe:H module is better than that of the CIS module at these high irradiance and low AM conditions

To compare the I-V characteristics of these modules under different spectral conditions, the above measurements were repeated at 17h30 on the same day (14 September). Figure 14 shows the normalized I-V characteristics of the same modules of Figure13 but measured at 17h30. The solar altitude was then estimated to be 15° corresponding to AM 3.9 from Equation (3). The modules were directed towards the sun to ensure high irradiance levels so as to allow reasonable comparison to the data presented in Figure 12. The average irradiance was 788 W/m^2 and the average back-of-module temperature 31°C.

From the figure it is evident that the normalized I-V characteristics of the CIS and a-SiGe:H modules are much closer here than at the lower AM values of Figure 10. This is attributed to the fact that the CIS module responds better to longer wavelength photons (associated with high AM values) than the a-SiGe:H module. The a-SiGe:H module, with its three different bandgap junctions, becomes less efficient when AM conditions move away from the AM 1.5 global spectrum since it was optimized at the latter. This is in accordance with the normalized I_{sc} values shown in Figure 11 and results obtained by other research groups (Eke & Senturk, 2013; King et al., 2000; Kipp & Zonen, 2012; Nazeeruddin et al., 1993; Rodziewicz et al., 2001; S. D. Studio, 2000), but contrary to results of van Cleef et. al. (2001).

Figure 15 gives the percentage difference between the maximum power and efficiency measured at 12h30 and that measured at 17h30. The percentage difference was determined with respect to the measurements taken at 12h30. The power of all modules decreased mainly due to the reduction in irradiance from 1100 W/m^2 to 788 W/m^2. The powers of the a-Si and a-SiGe:H modules decreased by 45% and 35%, respectively.

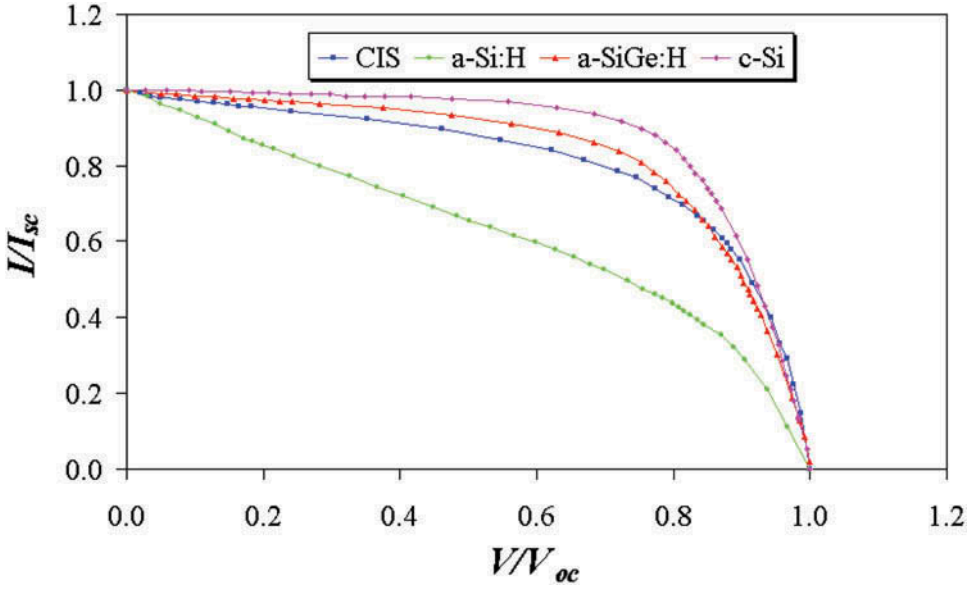

Figure 13. Normalized I-V characteristics measured close to solar noon (12h30) on 14 September.

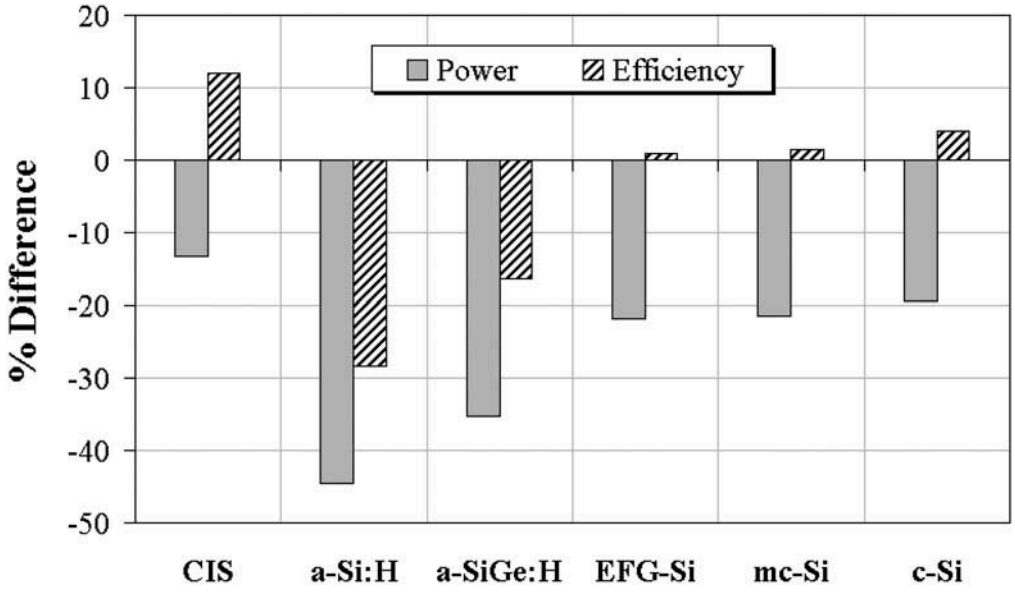

Figure 14. Percentage difference between the measurement of P_{max} and η taken at 12h30 and at 17h30.

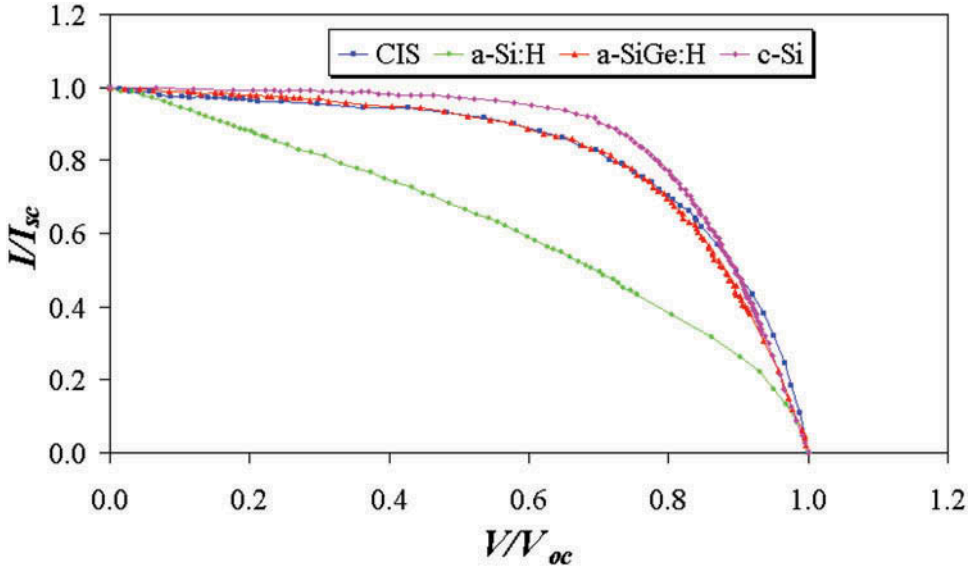

Figure 15. Normalized I-V characteristics measured at 17h30 on 14 September.

Notable from the figure is the 12% increase in the conversion efficiency of the CIS module. Again, this is explained by the behavior of the CIS module depicted in Figure 11. The efficiencies of the a-Si modules decreased and that of the crystalline modules increased slightly. This increase in η is attributed to the fact that the crystalline modules are relatively independent of AM changes but strongly dependent on the temperature change from 35°C to 31°C. Also, from Figure 11 it is clear that the performance of the crystalline modules increases with increase in AM.

Figure 11 through 15 show that STC measurements are by no means capable of accurately specifying module outdoor performance and that it is of utmost importance to be able to determine the performance of PV modules under actual operating conditions and understand the effect of temperature, irradiance and spectral distribution.

3.4. Conclusions

This research is devoted to a comparison between the performance parameters of six different module technologies used in this study. Parameters obtained from STC measurements showed that, although c-Si had the highest STC power, EFG-Si had the best quality cells. This was confirmed by V_{oc}-I_{sc} measurements from which ideality factor and saturation current could be obtained.

A comparison between the temperature dependence of the various technologies revealed that the crystalline technologies (EFG-Si, mc-Si and c-Si) are more temperature sensitive than their thin-film (CIS, a-Si:H and a-SiGe:H) counterparts. It is, therefore, concluded that the higher the quality of the module cells, the more sensitive it is to temperature changes.

Conversion efficiencies measured under reduced simulated light, showed that the a-Si:H technology is at least 16% more efficient than the other technologies at 169 W/m^2. This is due to recombination of e-h pairs being the dominant current dissipater. The outdoor performance of these technologies was then compared.

Unlike reduced simulated light, changes in the outdoor irradiance are associated with changes in the relative spectral content of natural sunlight. Results obtained indicate that CIS performs relatively better at high AM conditions, which are associated with red sunsets and times of day when the sun is lower in the sky. I-V characteristics measured at different times of day revealed that CIS was 12% more efficient at 17h30 than at 12h30. The efficiencies of the a-Si modules decreased significantly by up to 45% from 12h30 to 17h30.

In this research it was therefore shown that, although STC is an excellent way of comparing PV modules under specific reference conditions, it is by no means accurate in specifying the outdoor performances. Temperature, irradiance and spectral changes affect module performance. It is, therefore, essential to have actual data available of the outdoor performance of PV modules as well as the operating conditions.

Nomenclature

a-SiGe:H	aSi:H/a-SiGe:H/a-SiGe:H
CIS	$CuInSe_2$
EFG-Si	Edge-defined film-fed growth silicon
mc-Si	Multi-crystalline silicon
c-Si	Single crystalline silicon
SCR	Space-charge-region
n	Ideality factor
P_{max}	Maximum power
I_0	Saturated current
I_{sc}	Short-circuit current
I_{ph}	Photogenerated current
V_{oc}	Open-circuit voltage
FF	Fill factor
R_s	Series resistance
R_{sh}	Shunt resistance
η	Aperture area efficiency
α	Temperature coefficient for short-circuit current
β	Temperature coefficient for open-circuit voltage

γ Temperature coefficient for maximum power

Funding
This work was based on the research supported in part by the National Research Foundation of South Africa (Grant number GUN 86187, 116763). We also thank the Department of Science and Innovation, Eskom (TESP) and Govan Mbeki Research and Development Centre for supporting this research.

Author details
Edson L. Meyer[1]
E-mail: emeyer@ufh.ac.za
ORCID ID: http://orcid.org/0000-0002-9912-311X
Ochuko K. Overen[1]
E-mail: ooveren@ufh.ac.za
ORCID ID: http://orcid.org/0000-0003-4680-2626
[1] Institute of Technology, University of Fort Hare, Alice 5700, South Africa.

Cover
source:

Citation information
Cite this article as: Blue skies and red sunsets: Reliability of performance parameters of various p-n junction photovoltaic module technologies, Edson L. Meyer & Ochuko K. Overen, *Cogent Engineering* (2019), 6: 1691805.

References

Adeeb, J., Farhan, A., & Al-Salaymeh, A. (2019). Temperature effect on performance of different solar cell technologies. *Journal of Ecological Engineering*, *20*(5), 249–254. doi:10.12911/22998993/105543

Adrada Guerra, T., Amador Guerra, J., Orfao Tabernero, B., & de la Cruz García, G. (2017). Comparative energy performance analysis of six primary photovoltaic technologies in Madrid (Spain). *Energies*, *10*(6), 772. doi:10.3390/en10060772

Calzolari, P. U., & Graffi, S. (1972). A theoretical investigation on the generation current in silicon pn junctions under reverse bias. *Solid-state Electronics*, *15* (9), 1003–1011. doi:10.1016/0038-1101(72)90143-8

Carr, A. J., & Pryor, T. L. (2004). A comparison of the performance of different PV module types in temperate climates. *Solar Energy*, *76*(1), 285–294. doi:10.1016/j.solener.2003.07.026

Dai, Y., Huang, Y., He, X., Hui, D., & Bai, Y. (2019). Continuous performance assessment of thin-film flexible photovoltaic cells under mechanical loading for building integration. *Solar Energy*, *183*, 96–104. doi:10.1016/j.solener.2019.03.018

Das, G., De, M., & Mandal, K. K. (2019). PV array's resistance and temperature sensitivity analysis with shading effects. In *Proceeding of the Second International Conference on Microelectronics, Computing & Communication Systems (MCCS 2017)* (pp. 509–524), Jharkhand, India.

Del Cueto, J. A., Rummel, S., Kroposki, B., Osterwald, C., & Anderberg, A. (2008). Stability of CIS/CIGS modules at the outdoor test facility over two decades. In *Photovoltaic Specialists Conference, 2008. PVSC'08. 33rd* (pp. 1–6). IEEE, San Diego, USA.

Dubey, S., Sarvaiya, J. N., & Seshadri, B. (2013). Temperature dependent photovoltaic (PV) efficiency and its effect on PV production in the world–A review. *Energy Procedia*, *33*, 311–321. doi:10.1016/j.egypro.2013.05.072

Eke, R., & Betts, T. R. (2017). Spectral irradiance effects on the outdoor performance of photovoltaic modules. *Renewable and Sustainable Energy Reviews*, *69*, 429–434. doi:10.1016/j.rser.2016.10.062

Eke, R., & Senturk, A. (2013). "Monitoring the performance of single and triple junction amorphous silicon modules in two building integrated photovoltaic (BIPV) installations," Appl. *Energy*, *109*, 154–162.

Friesen, G., Zaaiman, W., & Bishop, J. (1998). Temperature behaviour of photovoltaic parameters. In *Proceedings 2nd World conference PVSEC* pp. 2392–2395

Hauser, J. R., & Ahmed, K. (1998). Characterization of ultra-thin oxides using electrical CV and IV measurements. *AIP Conference Proceedings*, *449*(1), 235–239.

Heise, G., Dickmann, M., Domke, M., Heiss, A., Kuznicki, T., Palm, J., & Huber, H. P. (2011). Investigation of the ablation of zinc oxide thin films on copper–Indium-selenide layers by ps laser pulses. *Applied Physics A*, *104*(1), 387–393. doi:10.1007/s00339-010-6159-1

Hishikawa, Y., Yoshita, M., Ohshima, H., Yamagoe, K., Shimura, H., Sasaki, A., & Ueda, T. (2018). Temperature dependence of the short circuit current and spectral responsivity of various kinds of crystalline silicon photovoltaic devices. *Japanese Journal of Applied Physics*, *57* (8S3), 08RG17. doi:10.7567/JJAP.57.08RG17

Hoseinzadeh, S., Ghasemiasl, R., Bahari, A., & Ramezani, A. H. (2017). The injection of Ag nanoparticles on surface of WO3thin film: Enhanced electrochromic coloration efficiency and switching response. *Journal of Materials Science: Materials in Electronics*, *28*(19), 14855–14863. doi:10.1007/s10854-017-7357-9

Hoseinzadeh, S., Ghasemias, R. l, Bahari, A., & Ramezani, A. H. (2018). Effect of post-annealing on the electrochromic properties of layer-by-layer arrangement FTO-WO3-Ag-WO3-Ag. *Journal of Electronic Materials*, *47*(7), 3552–3559. doi:10.1007/s11664-018-6199-4

Islam, M., Shawon, M. M. H., Akter, S., Chowdhury, A., Khan, S. I., & Rahman, M. M. (2019). Performance investigation of poly Si and mono Si PV modules: A comparative study In *2019 International Conference on Energy and Power Engineering (ICEPE)* (pp. 1–5), Dhaka, Bangladesh.

King, D. L., Kratochvil, J. A., & Boyson, W. E. (2000). Stabilization and performance characteristics of commercial amorphous-silicon PV modules. In *Photovoltaic Specialists Conference, 2000* (pp. 1446–1449). Conference Record of the Twenty-Eighth IEEE, Anchorage, USA.

Kipp & Zonen. (2012). *Solar monitoring stations*. Milan: Author.

Mattei, M., Notton, G., Cristofari, C., Muselli, M., & Poggi, P. (2006). Calculation of the polycrystalline PV module temperature using a simple method of energy balance. *Renewable Energy*, *31*(4), 553–567. doi:10.1016/j.renene.2005.03.010

Mazer, J. A. (1997). *Solar cells: An introduction to crystalline photovoltaic technology*. Norwell, USA: Kluwer Academic Publishers.

McMahon, T. J., Basso, T. S., & Rummel, S. R. (1996). Cell shunt resistance and photovoltaic module performance," in *Photovoltaic Specialists Conference, 1996* (pp. 1291–1294). Conference Record of the Twenty Fifth IEEE, Washington, USA.

Meyer, E. L. (2017). Extraction of saturation current and ideality factor from measuring Voc and Isc of photovoltaic modules. *International Journal of Photoenergy*, (12), 1–9. doi:10.1155/2017/8479487

Meyer, E. L., & Van Dyk, E. E. (2000). Degradation analysis of silicon photovoltaic modules. In *Proceedings of the 16th European photovoltaic solar energy conference*, Glasgow.

Meyer, E. L., & Van Dyk, E. E. (2004). Assessing the reliability and degradation of photovoltaic module performance parameters. *IEEE Transactions on Reliability*, *53*(1), 83–92. doi:10.1109/TR.2004.824831

Mousazadeh, H., Keyhani, A., Javadi, A., Mobli, H., Abrinia, K., & Sharifi, A. (2009). A review of principle and sun-tracking methods for maximising solar systems output. *Renewable and Sustainable Energy Reviews*, *13*(8), 1800–1818. doi:10.1016/j.rser.2009.01.022

Nazeeruddin, M. K., Kay, A., Rodicio, I., Humphry-Baker, R., Mueller, E., Liska, P., ... Graetzel, M. (1993). Conversion of light to electricity by cis-X2bis (2, 2′-bipyridyl-4, 4′-dicarboxylate) ruthenium (II) charge-transfer sensitizers (X= Cl-, Br-, I-, CN-, and SCN-) on nanocrystalline titanium dioxide electrodes. *Journal of the American Chemical Society*, *115*(14), 6382–6390. doi:10.1021/ja00067a063

Ogbomo, O. O., Amalu, E. H., Ekere, N. N., & Olagbegi, P. O. (2018). Effect of operating temperature on degradation of solder joints in crystalline silicon photovoltaic modules for improved reliability in hot climates. *Solar Energy*, *170*, 682–693. doi:10.1016/j.solener.2018.06.007

Omazic, A., Oreski, G., Halwachs, M., Eder, G. C., Hirschl, C., Neumaier, L., ... Erceg, M. (2019). Relation between degradation of polymeric components in crystalline silicon PV module and climatic conditions: A literature review. *Solar Energy Materials and Solar Cells*, *192*, 123–133. doi:10.1016/j.solmat.2018.12.027

Paul, D. I., Smyth, M., & Zacharopoulos, A. (2019). The effect of non-uniformities in temperature on the performance parameters of an isolated cell photovoltaic module with a compound parabolic concentrator. *International Journal of Renewable Energy Technology*, *10*(1–2), 3–25. doi:10.1504/IJRET.2019.097009

Perraki, V., & Tsolkas, G. (2013). Temperature dependence on the photovoltaic properties of selected thin-film modules. *International Journal of Renewable and Sustainable Energy*, *2*(4), 140. doi:10.11648/j.ijrse.20130204.12

Rodziewicz, T., Zabkowska-Waclawek, M., & Zdanowicz, T. (2001). Performance of PV modules fabricated in different technologies at strongly changeable insolation conditions. In *17th European photovoltaic solar energy conference*, Munich, Germany (pp. 540–543).

S. D. Studio. (2000). Sandia photovoltaic performance model-IV tracer v1. 0. *Maui Solar Energy Software Corporation*. Haiku, HI

Santhakumari, M., & Sagar, N. (2019). A review of the environmental factors degrading the performance of silicon wafer-based photovoltaic modules: Failure detection methods and essential mitigation techniques. *Renewable and Sustainable Energy Reviews*, *110*, 83–100. doi:10.1016/j.rser.2019.04.024

Singh, P., & Ravindra, N. M. (2012). Temperature dependence of solar cell performance—An analysis. *Solar Energy Materials and Solar Cells*, *101*, 36–45. doi:10.1016/j.solmat.2012.02.019

Sze, S. M., & Ng, K. K. (2006). *Physics of semiconductor devices*. New Jersey, USA: John wiley & sons.

Tang, W., Yang, K., He, J., & Qin, J. (2010). Quality control and estimation of global solar radiation in China. *Solar Energy*, *84*(3), 466–475. doi:10.1016/j.solener.2010.01.006

Van Cleef, M., Lippens, P., & Call, J., (2001). Superior energy yields of UNI-SOLAR® triple junction thin film silicon solar cells compared to crystalline silicon solar cells under real outdoor conditions in Western Europe. In *17th European photovoltaic solar energy conference and exhibition* (pp. 22–26), Munich, Germany.

Van Dyk, E. E., Meyer, E. L., Leitch, A. W. R., & Scott, B. J. (2000). Temperature dependence of performance of crystalline silicon photovoltaic modules. *South African Journal of Science*, *96*(4), 1-12.

Vázquez, M., & Rey-Stolle, I. (2008). Photovoltaic module reliability model based on field degradation studies. *Progress in Photovoltaics: Research and Applications*, *16*(5), 419–433. doi:10.1002/pip.v16:5

Zhukov, A. V. (2016). The effect of the electron–Phonon interaction on reverse currents of GaAs-based p–N junctions. *Semiconductors*, *50*(13), 1734–1737. doi:10.1134/S1063782616130145

***Cogent Engineering* (ISSN: 2331-1916) is published by Cogent OA, part of Taylor & Francis Group.**